

Development of a Biosorbent for Arsenite: Structural Modeling Based on X-ray Spectroscopy

MÔNICA CRISTINA TEIXEIRA[†] AND VIRGÍNIA S. T. CIMINELLI*

Department of Metallurgical and Materials Engineering, Federal University of Minas Gerais, Rua Espirito Santo 35-Cep 30161-030, Belo Horizonte MG, Brazil

This work describes a biological route for direct sorption of aqueous As(III) species, which are the most toxic and mobile arsenic species found in soils. Based upon the biochemical mechanisms that explain arsenic toxicity, we propose that a waste biomass with a high fibrous protein content obtained from chicken feathers can be used for selective As(III) adsorption. Prior to adsorption, the disulfide bridges present in the biomass are reduced by thioglycolate. Our investigations demonstrated that As(III) is specifically adsorbed on the biomass and, contrary to the behavior observed with inorganic sorbents, the lower is the pH the more effective is the removal. Arsenic uptake reaches values of up to 270 $\mu\text{mol As(III)}/\text{g}$ of biomass. Analyses by synchrotron light techniques, such as XANES, demonstrated that arsenic is adsorbed in its trivalent state, an advantage over conventional techniques for As uptake, which usually require a previous oxidation stage. EXAFS analyses showed that each As atom is directly bound to three S atoms with an estimated distance of 2.26 Å. The uptake mechanism is explained in terms of the structural similarities between the As(III)–biomass complex structure and that of arsenite ions and Ars-Operon system encoded proteins and phytochelatin. The biological route presented here offers the perspective of a direct removal of arsenic in its reduced form.

Introduction

Arsenic and its compounds are toxic and carcinogenic to all living organisms. Arsenic naturally occurs on the earth's crust in small concentrations, arsenopyrite (FeAsS) being the most common arsenic mineral (1). In soils, arsenic concentration may vary from 1.0 mg/kg (apatite, fluorite, and calcite samples) to 77 000–126 000 mg/kg (pyrite or arsenopyrite samples) (2). Typical arsenic concentration found in soils is reported at 6 mg/kg. Small amounts of arsenic and its compounds are utilized by the chemical and electronic industries to produce components for laser equipment, wood preservatives, pesticides, and glasses, to name but a few of the numerous applications. Despite its many applications, there is a surplus of arsenic-containing wastes, derived mainly from the mineral and metallurgical industries. The wastewater and solid residues produced by these industries are important potential sources for arsenic contamination

of surface and groundwater. Natural leaching of As-enriched soils and rocks has been the main cause for the arsenic contamination reported worldwide, such as in Canada, the United States, Chile, Argentina, China, India, and Bangladesh (1, 2).

The toxicity of arsenic and its compounds is well established (3, 4). Once ingested, arsenic provokes nausea and gastrointestinal symptoms. From the toxicological point of view, As(V) causes adverse effects to human and other living organisms due to its chemical similarity with phosphate (4, 5). In this case, arsenic poisoning can be reverted by the administration of an excess of phosphate. On the other hand, the trivalent species As(III) strongly binds to the sulfhydryl (SH) groups in the active sites of some dehydrogenases enzymes such as pyruvate and α -ketoglutarate, or dihydro-lipoate, causing irreversible metabolic impairments and, in some cases, cellular mutagenesis (6, 7), which therefore explains the higher toxicity of this species. The recognition that even trace amounts of arsenic, after long exposure, may cause severe health problems, such as dermatosis and cancer, has motivated a decrease in international limits for soluble arsenic in drinking water. Following recommendations from the World Health Organization, this limit has been reduced from 50 to 10 $\mu\text{g}\cdot\text{L}^{-1}$ in many countries.

Recent disasters involving cases of human poisoning due to arsenic contamination in drinking water, particularly in India and Bangladesh (8, 9), have spawned a series of worldwide investigations toward arsenic remediation. The episodes in the Asian countries are considered the most severe in terms of the extent of contamination and the number of persons affected (8–10). It has been estimated that more than 25 million people have been exposed to water with arsenic concentration $\geq 50 \mu\text{g}\cdot\text{L}^{-1}$ in West Bengal (India) and Bangladesh (11).

Immobilization and stability of arsenic species in natural environments or under remediation procedures are influenced by its oxidation state. The predominant water-soluble species are the As(III) and As(V) derivatives of the arsenous (H_3AsO_3) and arsenic (H_3AsO_4) acids, respectively. The trivalent species is of great environmental concern not only because of its considerably higher toxicity but also in view of its higher mobility in soils. Even under oxic conditions, both arsenic species occur together due to the fact that As(III) oxidation to As(V) is a kinetically slow process (12). In biological environments, bacterial activity can reduce As(V) species (3, 13), thus increasing arsenic toxicity. In the pentavalent state, arsenic acid (H_3AsO_4) species form stable surface complexes with soil constituents containing ferric, manganese, or aluminum oxy-hydroxides, such as goethite, alumina, hematite, birnessite, and gibbsite (2, 14–17), which explains its lower environmental mobility. On the other hand, the trivalent arsenous acid (H_3AsO_3) species are weakly bound to inorganic sorbents regardless of the pH. It is normally assumed that, to achieve high efficiency during arsenic remediation processes, such as precipitation as arsenic ferrihydrite or adsorption on iron (oxy)hydroxides, it is necessary to promote the oxidation of As(III) ions to As(V). Therefore, the conventional techniques used for As immobilization usually require a previous oxidative stage (9, 10). Therefore, those processes can be classified as As(V) removing systems.

Biosorption has been investigated by many as an alternative to conventional techniques for metal remediation. The predominant uptake mechanism usually involves unspecific ion exchange reactions. For instance, positively charged groups present in the biomass structure, such as the amino

* Corresponding author phone: 55 31 3238-1804; fax: 55 31 3238-1815; e-mail: ciminelli@demet.ufmg.br.

[†] Permanent address: Department of Pharmacy, Federal University of Ouro Preto, Brazil.

groups, are potential reactive sites to form adsorptive complexes with negatively charged ions, such as arsenate, arsenite, chromate, sulfate, or phosphate (18). Despite the identification of a number of biosorbents capable of removing a variety of species from aqueous solutions, the process often lacks selectivity in industrial complex, multicomponent systems. We believe that the poor selectivity associated with unspecific ion exchange mechanisms has been one of the main limitations hindering biosorption's commercial applications.

The present work aims at designing a specific biosorbent for arsenic, with an approach based on the following premises: (i) the toxicity of As(III) is considerably higher when compared to As(V), (ii) this higher toxicity may be explained in terms of the great chemical affinity that exists between As(III) and the sulfhydryl groups, and (iii) the As(V) affinity for sulfhydryl groups is lower when compared to As(III).

Based on the previous considerations, a waste biomass with a high fibrous protein content provided by the poultry industry was selected and tested for As(III) sorption. The biomass is a keratin-rich material. Keratin is a fibrous protein, which contains cysteine amino acid residues in its primary structure; the lateral group of each cysteine molecule is the sulfhydryl (SH) group. Two cysteine molecules may react forming a cystine molecule, which is, in fact, a molecule with two cysteine residues bound by a disulfide bridge. Thioglycolate is a reduction agent that reacts with the disulfide bridge, restoring the SH groups. Our selection of this specific biomass was based on its cysteine content.

Supported by the results shown in the following paragraphs, the specificity of the selected biosorbent for As(III) is demonstrated. This feature is explained by the molecular structure of the adsorbed complex determined by synchrotron light, X-ray spectroscopy analyses.

Materials and Methods

Biomass Preparation. White chicken feathers were rinsed thoroughly with warm tap water and dried at 45 ± 5 °C for 24 h. The dried material was ground and sieved to obtain a size range below 0.037 mm (400 Mesh Tyler). Biomass activation was accomplished by adding 10 mL of a 7.8% (w/w) basic ammonium thioglycolate solution. Treatment did not imply any mass loss. After this activation step, the powdered biomass was filtered, washed with 100 mL of Milli-Q water, and used in the adsorption tests.

Materials. All solutions were prepared with analytical grade chemicals and Milli-Q water. As(III) stock solutions of 10 000 mg/L were prepared with AsNaO₂ (Fluka, 99.0%) salt. The pH values were adjusted with 0.1 N HCl or NaOH solutions; E_h was constantly monitored by means of a platinum Ag/AgCl electrode. Ionic strength (I) was fixed by using 4 mol/L NaCl or 0.01 mol/L Na₃PO₄ electrolyte solutions.

Adsorption Experiments. As(III) batch adsorption experiments were conducted at room temperature (28 ± 3 °C), by adding a known amount of biosorbent (1–10 mg/L) to each 250-mL Erlenmeyer flask containing the As solution (100 mL). Flasks were shaken (100 rpm) for 1 h to achieve equilibrium. As(III) semicontinuous adsorption experiments were undertaken at a constant temperature (25 ± 0.2 °C) using an apparatus similar to that described by Pagnanelli et al. (19), as the "Subsequent Additions Method" or SAM. The procedure consists of successive additions of a concentrated heavy metal solution to a biomass suspension kept under agitation and constant pH (by addition of NaOH or HCl solutions). The concentrated metal solution is added to the cell suspension in time intervals; after 60 min (equilibrium time) of each addition, a 10 mL sample was collected for analyses. The liquid volume in the reactor was 1000 mL, the

biosorbent concentration was 2 g/L, and agitation and pH values were kept constant. Reaction suspensions were filtered through a 0.45 μ m cellulose membrane and were preserved with concentrated nitric acid (5 μ L) for chemical analyses by AAS. Experiments were carried out in duplicate, and results were averaged; experimental errors were below 10%.

XANES and EXAFS Analyses. X-ray absorption near edge structure (XANES) and extended X-ray absorption fine structure (EXAFS) analyses of wet biomass samples loaded with As(III) were performed using the synchrotron facilities at the Laboratório Nacional de Luz Síncrotron (LNLS), in Campinas, Brazil. XANES and EXAFS data from the arsenic K edge (11 868 eV) were obtained at XAS workstation, under operation conditions of 1.37 GeV and beam currents of about 200 mA. All spectra were recorded at room temperature using a Si (111) double crystal monochromator with an upstream vertical aperture of 0.6 mm. Arsenic K-edge X-ray absorption spectra were measured by monitoring the transmitted energy using a 15-element Ge detector (Canberra Industries). Solid samples were fixed onto steel holders, sealed with Kapton tape film, and placed at an angle of 45° to the incident beam. The energy resolutions utilized were 0.8 eV at the XANES region (11 855–11 930 eV), 2 eV between 11 760 and 11 855 eV, and 11 930 and 12 400 eV, and 3 eV in the 12 400–13 000 eV region. XANES and EXAFS spectra were obtained simultaneously. Counting times of 3 s were kept constant. XANES spectra were analyzed using the Origin 6.0 software, and collected data from EXAFS were analyzed by using the Winxas 2.0 software. EXAFS data fit was obtained using phase and amplitude parameters calculated with the FEFF 6.01 software.

Results and Discussion

There is a limited number of biosorbents specially developed for arsenic. Examples such as MICB (molybdate-impregnated chitosan beads) (20) are usually more effective in removing the pentavalent species, and, as for the inorganic sorbents (i.e., goethite, alumina, gibbsite, and ferric oxides), it is often necessary to oxidize the trivalent arsenic to favor its immobilization. Arsenite uptake by inorganic sorbents is usually favored at high pH, while arsenate uptake is favored at low pH. Oxyanions often exhibit adsorption maxima at pH value close to the pK_a of their first dissociation constant (21). Therefore, for the As(III) species, this would imply a maximum adsorption at pH close to 9, and for the arsenate species at pH close to 2. The development of a specific biosorbent for As(III) removal from dilute aqueous solutions took into account the mechanism that explains the toxicity of arsenic species, that is, irreversible enzymatic inhibition caused by the reaction of As(III) with cysteine sulfhydryl groups. Therefore, the use of a cysteine-rich biomass, as found in animal skin, hair, nails, horns, or feathers, has been proposed. Chicken feathers were finally selected in view of their abundance as a waste residue from the poultry industry.

Preliminary experimental results related to As(III) adsorption by the selected biomass are shown in Table 1 and Figure 1. The results shown in Table 1 confirm the role of sulfhydryl reduced groups on arsenic adsorption (tests A and D) and also allow for the evaluation of possible loss of arsenic caused by precipitation with thioglycolate or adsorption onto filtration membranes (A and B). For those purposes, an excess of thioglycolate (10 times greater than that used in the actual activation procedure) was intentionally used; the results suggest no removal of arsenic by precipitation with the reagent. Experiments performed with biomass prior to the activation reaction with thioglycolate solution led to a negligible As uptake. This finding supports the hypothesis that the reduced sulfhydryl groups are responsible for arsenic adsorption. Arsenite adsorption onto nonactivated biomass is insignificant and similar to that obtained with the cellu-

TABLE 1. Effect of Pretreatment on As(III) and As(V) Removal

test	biomass	thioglycolate solution (%)	pretreatment (min)	As(III) removal (%)	As(V) removal (%)
A	+	10	60	29.3	6.1
B	+	10	60	29.9	5.5
C	-			4.0	0
D	+			3.9	0

Powdered biomass concentration, 1 g/L; (I = 0, 1; Initial As concentration = 2.67 mmol.L⁻¹ (200 ppm); pH 5.0; Equilibrium time, 1 hour; Temperature, 25 °C; shaker, 150 rpm. (a) Biomass pre-treated with thioglycolate solution for one hour; material filtered through a 0.45 μm acetate cellulose membrane; (b) Biomass pre-treated with thioglycolate solution for one hour, material not filtered; (c) Flasks containing only a 0.45 μm acetate cellulose membrane; (d) Flasks containing only raw, ground biomass.

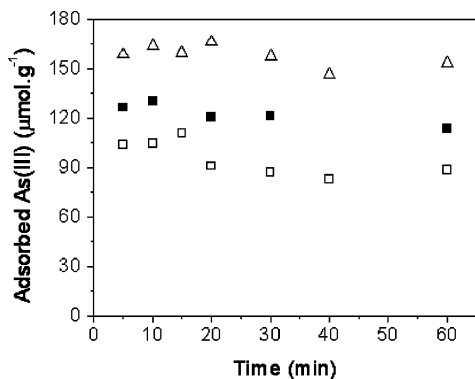


FIGURE 1. As(III) uptake by powdered biomass, 2 g L⁻¹ (Δ), 1 g L⁻¹ (□), and whole biomass, 1 g L⁻¹ (■). Flask tests, As(III) initial concentration, 1.34 mmol L⁻¹; initial pH, 9.2; temperature, 28 ± 3 °C; pretreatment, 2 h.

lose acetate membrane (C). The biomass selectivity toward As(III) is clearly demonstrated.

Because the experimental conditions were strongly reductive, the formation of volatile arsine (AsH₃) or solid compounds such as realgar (As₂S₂) or orpiment (As₂S₃) was also a matter of concern. According to the E_h versus pH diagram for the As-S-H₂O system (22, 23), reduction of As³⁺ to As³⁻ is only achieved at E_h < 0 V and therefore at redox potentials considerably lower than the lowest E_h of 297 mV determined during the experiments. In a broad pH range (from 2.0 to 10.0) and even with the thioglycolate concentration 10 times greater than that used in the activation protocol, no loss of arsenic by volatilisation or precipitation was detected.

The As(III) adsorption on whole and powdered biomass was evaluated by the experiments described in Figure 1. The highest As uptake was obtained when waste-activated biomass was employed at the concentration of 2.0 g L⁻¹. The results obtained for powdered biomass were slightly lower than those obtained for whole biomass. Regardless of the biomass concentration, equilibrium was achieved in less than 10 min. The milling process seems to negatively contribute to As uptake. Nevertheless, all of the subsequent experimental tests were performed using ground material for the benefit of sample homogeneity.

The influence of pH on As(III) biosorption can be observed in Figure 2. Arsenic uptake at pH values of 2.0, 5.0, 8.0, and 10.0 were compared. During all of the adsorption experiments, pH variation was less than 0.2 units, thus indicating no net release of H⁺ or OH⁻ groups. The obtained results showed that the lower is the pH, the higher is the uptake. This trend is just the opposite of that observed for As(III) adsorption onto inorganic sorbents, for which uptake

increases with pH (16, 21, 24–27). Taking into account that the pK_{a1} for arsenous acid is 9.2, one can see that As(III) neutral species are preferably adsorbed by the biomass instead of the negatively charged ones. Arsine formation during sorption experiments carried out at pH 2.0 was experimentally investigated and also discarded.

To obtain the adsorption experimental parameters Q_{max} and k, the experimental data exhibited in Figure 2 were adjusted to a linear expression of the Langmuir equation:

$$C_{eq}q^{-1} = kQ_{max}^{-1} + C_{eq}Q_{max}^{-1} \quad (1)$$

where C_{eq} is the As equilibrium concentration in the aqueous phase.

Before the linearized Langmuir isotherms were adopted, the mathematical parameters obtained with and without linearization have been compared. A good fit and similar results were obtained in both cases (Figure 3). The obtained Q_{max} values were 173.6 and 135.1 μmol As(III) g⁻¹ at pH 2.0 and pH 5.0, respectively. The values for the constant k were 0.06 at pH 2.0 and 0.04 at pH 5.0; the calculated correlations factors were both above 0.996. Those values clearly demonstrated that As adsorption is favored at pH 2.0.

In 1930, Johnson and Voegtlin (23) described As/cysteine ML3 complexes. Their respective stability constants and the As(III)/Cys speciation diagrams were described later by Reyes (28) and showed that at equal arsenic and cysteine concentrations (0.015 mol/L) almost 20% of the present As(III) atoms are complexed with almost 60% of the existent cysteine molecules at pH values between 2.5 and 7.0. The other 80% As remained as the neutral arsenic species, As(OH)₃. As pH increases and the hydroxyl concentration becomes greater, the negatively charged arsenic species As(OH)₂O⁻ are formed and the stoichiometry of the complexation reaction is changed. Now, hydroxyl groups compete with thiol groups, and, as a consequence, cysteine molecules are dislocated from the arsenic coordination shell. The resultant complex is the negatively charged [As(HCys)(OH)O]⁻. At pH 8–9.5, the predominant species is the negatively charged complex with an As/Cys proportion of 1:1. Both As/Cys complexes show trigonal-pyramidal geometry. However, in the negatively charged complex, the arsenic inner coordination shell involves two hydroxyl groups as ligands, one of them in a nonprotonated form (28).

Experimental data obtained for arsenic adsorption at pH values higher than 5.0 corroborate those theoretical considerations (Figure 2). At pH 8 and 10, As uptakes are lower relative to those obtained under more acidic conditions, and the data are not fitted by the Langmuir equation. This behavior can be explained by the fact that at pH 8 and 10, the neutral arsenic species are replaced by the anionic species, producing different adsorption complexes.

Arsenic uptake (Q_{max}) of 173.6 or 135.1 μmol g⁻¹ obtained at pH 2.0 and 5.0, respectively, is promising and greater than those values obtained with kaolinite and montmorillonite, 1.33 and 2.66 μmol g⁻¹, respectively (29), alumina, 2.66 μmol g⁻¹ (16), and goethite, 39.9 μmol g⁻¹ (15). Ladeira et al. (14), report significant uptakes by thermally activated gibbsite, 337.82 μmol g⁻¹. Driehaus et al. (17), and Meng et al. (30), also obtained higher arsenic adsorption capacities (266–532 μmol g⁻¹), but, in both cases, As(III) was previously oxidized to As(V). The very high value (920.4 μmol of As(III) per gram of Mo) reported by Dambies et al. (20), using a chitosan derivative biosorbent impregnated with molybdenum, cannot be compared to other reported results in view of the lack of information with regard to the used quantities (mass) of biosorbent.

Despite the best adsorption capacity achieved at pH 2.0, a pH of 5.0 was chosen for all of the subsequent experiments,

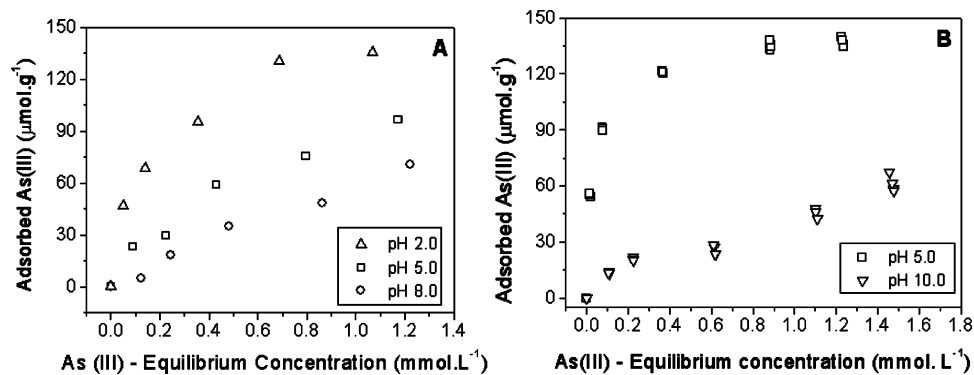


FIGURE 2. Influence of pH on As(III) adsorption: (A) SAM procedure, (B) flask tests (biomass, 2 g/L; temperature, $25 \pm 1^\circ\text{C}$).

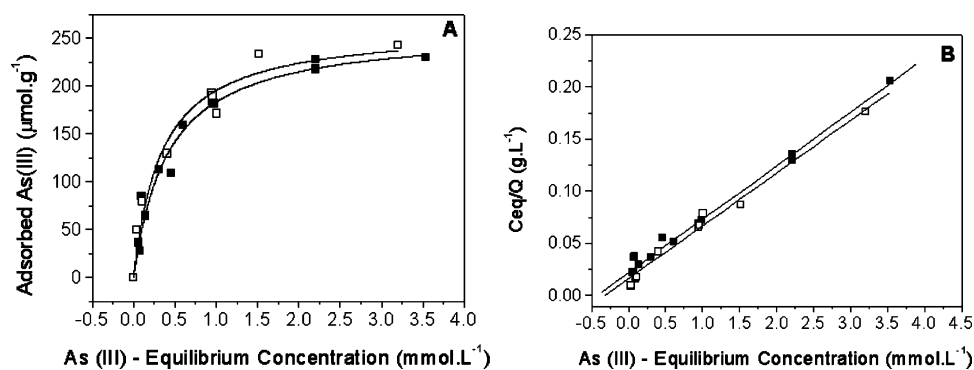


FIGURE 3. Influence of phosphate ions on As(III) adsorption isotherms in the presence (■) or in the absence (□) of phosphate 0.01 mol L^{-1} (SAM procedure, $I = 0.1$; pH = 5; biomass, 2 g/L; temperature, $25 \pm 1^\circ\text{C}$). Lines indicate the fit by the Langmuir equation.

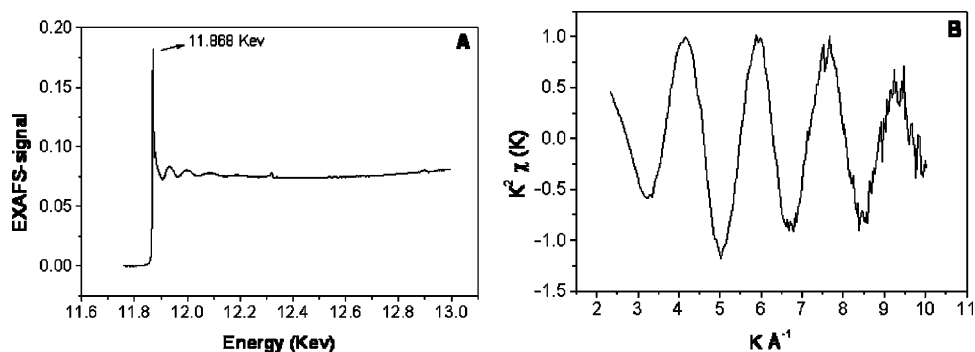


FIGURE 4. EXAFS signal of As(III) (AsNaO_2) adsorbed onto biomass, after background correction.

as this pH value is more consistent with conditions often found in natural wastewater.

The selectivity toward As(III), shown in Table 1, is corroborated by the results shown in Figure 3; the good fit of the experimental data to the linear form of Langmuir equation is also depicted (the calculated correlations factors were higher than 0.99). The great majority of As sorbents described in the literature are active for both the pentavalent and the trivalent species, the main difference being the relatively higher remobilization of the latter by aqueous solutions. Under conditions of pH 5.0, $I = 0.1$, biomass concentration of 2.0 g L^{-1} , the Q_{max} values obtained in the presence ($260.35 \mu\text{mol g}^{-1}$) and absence of phosphate ions (265.35 mol/L) are quite similar (Figure 3). Therefore, the well-described competition between arsenic and phosphate during sorptive experiments using biosorbents or resins (20, 31) is not observed when the fibrous protein-rich biomass is utilized for As(III) uptake.

Both phosphate and arsenate molecules have the same tetrahedral geometry, which could explain their chemical similarity and their similar affinities for the same chemical ligands. Conversely, arsenite ions possess a trigonal pyramidal

geometry. It is possible that a steric hindrance may contribute to the rejection of the tetrahedral arsenate and phosphate oxyanions by the biomass adsorptive sites.

X-ray absorption near edge structure (XANES) and extended X-ray absorption fine structure (EXAFS) provide information that could not be otherwise obtained through the traditional surface analyses techniques. XANES spectra offer electronic and structural information, such as oxidation state with regard to adsorbed ion (photoabsorbing ion). EXAFS provides information, for example, the coordination number and interatomic distance, and the nature and position of the neighbor atoms in the coordination shell of the photoabsorbing ion (arsenic, in our case). XANES and EXAFS made it possible to identify the variations inside the arsenic coordination shell caused by adsorption onto cysteine-rich biomass.

The analysis of the EXAFS data from the arsenite-loaded biomass is illustrated in Figures 4–6. The As (III)-biomass EXAFS spectrum is presented in Figure 4. The averaged data from seven different spectra were converted to an eV energy unit and then the background line was extracted. The experimentally obtained K edge value (E_0) was found as 11 868

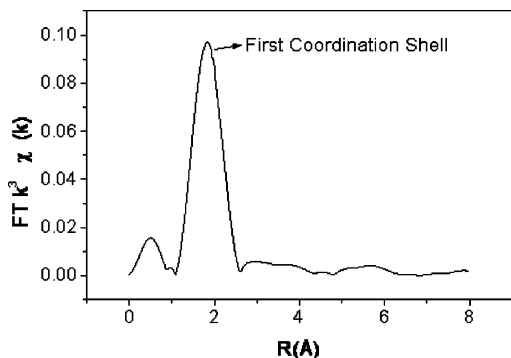


FIGURE 5. Fourier transform amplitude ($K = 3$). Radial distribution functions for As(III) adsorbed onto biomass.

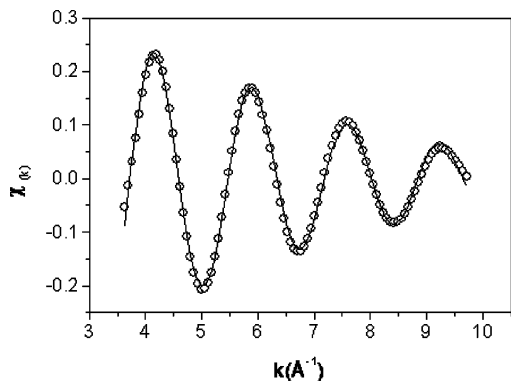


FIGURE 6. Back Fourier transform (K -space), first coordination shell. Best fit of EXAFS data to As(III) adsorbed on biomass. Experimental data were fitted to hypothetical As/S complex using FEFF 6.0. Scatter and line curves represent experimental and theoretical data, respectively. Structural parameters obtained are $R = 2.26 \pm 0.01 \text{ \AA}$, $n = 2.5 \pm 0.4$, $E_0 = 6.87$, and $\sigma^2 = 0.002$.

eV, the same obtained for the arsenite standard sample, confirming that arsenite was not oxidized by the biomass. XANES spectra (data not shown) validated this value and the trivalent state of arsenic atoms. The spectrum oscillations caused by all of the atoms in the neighboring coordination shells are also presented. This spectrum was submitted to Fourier transform, thus allowing the identification of one amplified peak that corresponds to the first arsenic coordination shell (Figure 5).

The signal obtained after submitting these data to another Fourier transform treatment results in one spectrum that represents only the oscillations caused by the atoms in the As first coordination shell. At this point, it is possible to calculate the structural parameters such as interatomic distance between As and atoms in the first coordination shell, coordination number, as well as to identify the “first neighbor” ligand. By adjusting the experimental data with the theoretical model provided by the FEFF program (Figure 6), it was possible to confirm that sulfur is the retro-scattering atom. It was also possible to determine that each arsenic atom is bound to three sulfur atoms. The final structural parameters obtained in the analyses were coordination number (n) = 2.52 ± 0.4 and interatomic distance (R) = $2.26 \pm 0.01 \text{ \AA}$.

The structural parameters obtained during this work are quite different from those obtained by arsenic adsorption on inorganic matrixes. As arsenic is adsorbed as an oxyanion, often as a bidentate binuclear complex, the element found in the first coordination shell is always oxygen, in coordination numbers (n) varying from 3.6 to 4, and interatomic (R) distances in a range of 1.72–1.78 Å. The metal ligands (Fe or Al) are found in the second coordination shell with R values often greater than 3.0 Å (32).

The coordination number and interatomic distance obtained in the present study are, as expected, very similar to those reported in EXAFS analyses of biological As(III)/protein complexes, showing As atoms directly bound to S atoms in the first coordination shell. Each As atom is bound to the sulfur atoms coming from three different cysteine residues, with R values vary from 2.2 to 2.25 Å (33–37). The information provided by XAS analyses is consistent with the strong arsenic uptake reported here. The results explain that, rather than adsorbed as a counterion, or specifically adsorbed as arsenous species in the inner Helmholtz plane, As(III) undergoes a chemical reaction leading to dehydration of H_3AsO_3 molecules.

On the basis of these findings, the following equation is proposed to describe arsenite adsorption by the fibrous protein biomass:



where B represents the biomass matrix.

This adsorption mechanism is supported by the structural similarities between the As(III)/biomass complex and those natural complexes formed between arsenic atoms and Ars Operon proteins (33, 34, 36–38), phytochelatins (35, 39), or cysteine and glutathione (3, 4, 13, 36), previously identified. Finally, it may be stressed that the adsorption phenomenon studied here involves a chemical reaction between the dissolved arsenite ions and the sulfhydryl groups of biomass, strong enough to dislocate oxygen atoms from the arsenic atom first coordination shell in arsenous acid molecules. These facts explain the specificity of this tested biosorbent with respect to the trivalent species of arsenic as well as its minor affinity for phosphate and arsenate ions. Our findings are consistent with the statements of Farrer (36): “As(III) is able to distort polypeptide structure in order to satisfy its desire to form trigonal-pyramidal thiolate coordination” and “Arsenic causes structural distortion and aggregation in biopolymers, an action which may be involved in the mechanism of arsenic toxicity.”

The features of the model proposed to explain As(III) adsorption onto the selected fibrous, protein-rich biomass can be summarized as follows. Sulfhydryl reduced groups are the active groups involved in arsenic biosorption. Uptake increases as pH decreases; phosphate ions do not compete with arsenite ions for the biomass’ active sites. Arsenic(III) uptake involves an inner-sphere complexation phenomenon that takes place within the As first coordination shell. Three water molecules are released, while the arsenic atom directly binds to the sulfhydryl groups. XAS analyses indicated that each arsenic atom is bound directly to three sulfur atoms from the reduced cysteine amino acids. The arsenic/sulfur interatomic distance was found to be $2.26 \pm 0.01 \text{ \AA}$. Finally, the specificity of the biosorbent dispenses the need for previous As(III) oxidation.

Acknowledgments

We thank the National Synchrotron Light Laboratory (LNLS) in Campinas, São Paulo, for the use of XAS facilities, the Brazilian Scholarship Program-PICD from CAPES, and Dr. Maria do Carmo Alves for her important technical support during XAS data analyses. We are also grateful to the Millennium Science Initiative, Water a mineral approach, and CNPq for their financial support.

Literature Cited

- (1) Mandal, B. K.; Suzuki, K. T. Arsenic round the world: a review. *Talanta* **2002**, *58*, 201–235.
- (2) Smedley, P. L.; Kinniburgh, D. G. A review of the source, behaviour and distribution of arsenic in natural waters. *Appl. Geochem.* **2002**, *17*, 517–568.

- (3) Knowles, F. C.; Benson, A. A. The biochemistry of arsenic. *Trends Biochem. Sci.* **1983**, *8*, 178–179.
- (4) Hughes, M. F. Arsenic toxicity and potential mechanisms of action. *Toxicol. Lett.* **2002**, *133*, 1–16.
- (5) Nies, D. H. Microbial heavy-metal resistance. *Appl. Microbiol. Biotechnol.* **1999**, *51*, 730–750.
- (6) Treagan, L. In *Methods Involving Metal Ions and Complexes in Clinical Chemistry*; Siegel, H., Ed.; Marcel Dekker: New York, 1983; Vol. 16, pp 47–83.
- (7) Flessel, P.; Furst, A.; Radding, S. B. In *Carcinogenicity and Metal Ions*; Siegel, H., Ed.; Marcel Dekker: New York, 1980; Vol. 10, pp 22–54.
- (8) Acharyya, S. K.; Chakraborty, P.; Lahiri, S.; Raymahashay, B. C.; Guha, S.; Bhowmik, A. Arsenic poisoning in the Ganges delta. *Nature* **1999**, *401* (7, October), 545.
- (9) Nickson, R.; McArthur, J.; Burgess, W.; Ahmed, K. M.; Ravenscroft, P.; Rahman, M. Arsenic poisoning of Bangladesh groundwater. *Nature* **1998**, *395* (24, September), 338.
- (10) Chowdhury, T. R.; Basu, G. K.; Mandal, B. K.; Biswas, B. K.; Samanta, G.; Chowdhury, U. K.; Chanda, C. R.; Lodh, D.; Roy, S. L.; Saha, K. C.; Roy, S.; Kabir, S.; Quamruzzaman, Q.; Chakraborti, D. Arsenic poisoning in the Ganges delta. *Nature* **1999**, *401* (7, October), 545–546.
- (11) Chakraborti, D.; Rahman, M. M.; Paul, K.; Chowdhury, U. K.; Sengupta, M. K.; Lodh, D.; Chanda, C. R.; Saha, K. C.; Mukherjee, S. C. Arsenic calamity in the Indian subcontinent. What lessons have been learned? *Talanta* **2002**, *58*, 3–22.
- (12) Weerasooriya, R.; Tobschall, H. J.; Wijesekara, H. K. D. K.; Arachchige, E. K. I. A. U. K.; Pathirathne, K. A. S. On the mechanistic modelling of As(III) adsorption on gibbsite. *Chemosphere* **2003**, *51*, 1001–1013.
- (13) Mukhopadhyay, R.; Rosen, B. P.; Phung, L. T.; Silver, S. Microbial Arsenic: from geocycles to genes and enzymes. *FEMS Microbiol.* **2002**, *26*, 311–325.
- (14) Ladeira, A. C. Q.; Ciminelli, V. S. T.; Duarte, H. A.; Alves, M. C. M.; Ramos, A. Y. Mechanism of anion retention from EXAFS and Density Functional Calculations: Arsenic (V) adsorbed on gibbsite. *Geochim. Cosmochim. Acta* **2001**, *65*, 1211–1217.
- (15) Deschamps, E.; Ciminelli, V.; Weidler, P. G.; Ramos, A. Y. Arsenic sorption onto soils enriched with manganese and iron minerals. *Clays Clay Miner.* **2003**, *51*, 198–205.
- (16) Gupta, S. K.; Chen, K. C. Arsenic removal by adsorption. *J. Water Pollut. Control Fed.* **1978**, *50*, 493–506.
- (17) Driehaus, W.; Seith, R.; Jekel, M. Oxidation of arsenate(III) with manganese oxides in water treatment. *Water Res.* **1995**, *29*, 297–305.
- (18) Veglio, F.; Beolchini, F. Removal of metals by biosorption: a review. *Hydrometallurgy* **1997**, *44*, 301–316.
- (19) Pagnanelli, F.; Papini, M. P.; Trifoni, M.; Toro, L.; Veglio, F. Biosorption of metals ions on *Arthrobacter* sp.: biomass characterization and biosorption modeling. *Environ. Sci. Technol.* **2000**, *34*, 301–316.
- (20) Dambies, L.; Vincent, T.; Guibal, E. Treatment of Arsenic-containing solutions using chitosan derivatives: uptake mechanism and sorption performances. *Water Res.* **2002**, *36*, 3699–3710.
- (21) Bostick, B. C.; Fendorf, S. Arsenite sorption on troilite (FeS) and pyrite (FeS₂). *Geochim. Cosmochim. Acta* **2003**, *67*, 909–921.
- (22) Vink, B. W. Stability relations of antimony and arsenic compounds in the light of revised and extended Eh-pH diagrams. *Chem. Geol.* **1996**, *130*, 21–30.
- (23) Johnson, J. M.; Voegtlin, C. Arsenic derivatives of cysteine. *J. Biol. Chem.* **1930**, *89*, 27.
- (24) Goldberg, S.; Johnston, C. T. Mechanisms of arsenic adsorption on amorphous oxides evaluated using macroscopic measurements, vibrational spectroscopy and surface complexation modelling. *J. Colloid Interface Sci.* **2001**, *234*, 204–216.
- (25) Dixit, S.; Hering, J. G. Comparison of arsenic(V) and arsenic(III) sorption onto iron oxide minerals: implications for arsenic mobility. *Environ. Sci. Technol.* **2003**, *37*, 4182–4189.
- (26) Ladeira, A. C. Q.; Ciminelli, V. S. T. Adsorption and desorption of arsenic on an oxisol and its constituents. *Water Res.* **2004**, *38*, 2087–2094.
- (27) Singh, T. S.; Pant, K. K. Equilibrium, kinetics and thermodynamic studies for adsorption of As(III) on activated alumina. *Sep. Purif. Technol.* **2004**, *36*, 139–1478.
- (28) Rey, N. A.; Howarth, O. W.; Maia, E. C. P. Equilibrium characterization of the As(III)-cysteine and the As(III)-glutathione systems in aqueous solution. *J. Inorg. Biochem.* **2004**, *98*, 1151–1159.
- (29) Griffin, R. A.; Frost, R. R.; Au, A. K.; Robinson, G. D.; Shimp, N. F. Attenuation of pollutants in municipal landfill leachate by clay minerals. *Environ. Geol. Notes* **1977**, *79*, 1–47.
- (30) Meng, X.; Korfiatis, G. P.; Bang, S.; Bang, K. W. Combined effects of anions on arsenic removal by iron hydroxides. *Toxicol. Lett.* **2002**, *133*, 103–111.
- (31) Korngold, E.; Belayev, N.; Aronov, L. Removal of arsenic from drinking water by anion exchangers. *Desalination* **2001**, *141*, 81–84.
- (32) Farquhar, M. L.; Charnock, J. M.; Livens, F. R.; Vaughan, D. J. Mechanisms of arsenic uptake from aqueous solution by interaction with goethite, lepidocrocite, mackinawite and pyrite: an X-ray absorption spectroscopy study. *Environ. Sci. Technol.* **2002**, *36*, 1757–1762.
- (33) Shi, W.; Dong, J.; Scott, R. A.; Kasenzenko, M. Y.; Rosen, B. The role of arsenic-thiol interactions in metalloregulation of the ars operon. *J. Biol. Chem.* **1996**, *271*, 9291–9297.
- (34) Bhattacharjee, H.; Rosen, B. Spatial proximity of Cys 113, Cys 172, and Cys 422 in the metalloactivation domain of the ArsAATPase. *J. Biol. Chem.* **1996**, *271*, 24465–24470.
- (35) Pickering, I. J.; Price, R. C.; George, M. J.; Smith, R. D.; George, G. N.; Salt, D. E. Reduction and coordination of arsenic in Indian mustard. *Plant Physiol.* **2000**, *122*, 1171–1177.
- (36) Farrer, B. T.; McClure, C. P.; Penner-Hahn, J. E.; Pecoraro, V. L. Arsenic(III)-Cysteine interactions stabilize three-helix bundles in aqueous solution. *Inorg. Chem.* **2000**, *39*, 5422–5423.
- (37) Martin, P.; DeMel, S.; Shi, J.; Gladysheva, T.; Gatti, D. L.; Rosen, B. P.; Edwards, B. F. P. Insights into the structure, solvation and mechanism of ArsC arsenate reductase, a novel arsenic detoxification enzyme. *Structure* **2001**, *9*, 1071–1081.
- (38) Kaur, P.; Rosen, B. P. Plasmid-Encoded resistance to arsenic and antimony. *Plasmid* **1992**, *27*, 29–40.
- (39) Schmoeger, M. E. V.; Oven, M.; Grill, E. Detoxification of arsenic by phytochelatins in plants. *Plant Physiol.* **2000**, *122*, 793–801.

Received for review March 30, 2004. Revised manuscript received October 19, 2004. Accepted October 27, 2004.

ES049513M